



City Research Online

City, University of London Institutional Repository

Citation: Lunt, S. J., Akerman, S., Hill, S. A., Fisher, M., Wright, V. J., Reyes-Aldasoro, C. C., Tozer, G. M. & Kanthou, C. (2011). Vascular effects dominate solid tumor response to treatment with combretastatin A-4-phosphate. *International Journal of Cancer*, 129(8), pp. 1979-1989. doi: 10.1002/ijc.25848

This is the accepted version of the paper.

This version of the publication may differ from the final published version.

Permanent repository link: <https://openaccess.city.ac.uk/id/eprint/28092/>

Link to published version: <https://doi.org/10.1002/ijc.25848>

Copyright: City Research Online aims to make research outputs of City, University of London available to a wider audience. Copyright and Moral Rights remain with the author(s) and/or copyright holders. URLs from City Research Online may be freely distributed and linked to.

Reuse: Copies of full items can be used for personal research or study, educational, or not-for-profit purposes without prior permission or charge. Provided that the authors, title and full bibliographic details are credited, a hyperlink and/or URL is given for the original metadata page and the content is not changed in any way.

City Research Online:

<http://openaccess.city.ac.uk/>

publications@city.ac.uk

Vascular effects dominate solid tumor response to treatment with combretastatin A-4-phosphate

Sarah Jane Lunt¹, Simon Akerman¹, Sally A. Hill², Matthew Fisher¹, Victoria J. Wright¹, Constantino C. Reyes-Aldasoro¹, Gillian M. Tozer¹ and Chryso Kanthou¹

¹ Cancer Research UK Tumour Microcirculation Group, Department of Oncology, School of Medicine, University of Sheffield, Sheffield, United Kingdom

² Radiobiology Research Institute, Churchill Hospital, Headington, Oxford, United Kingdom

Abstract: Vascular-targeted therapeutics are increasingly used in the clinic. However, less is known about the direct response of tumor cells to these agents. We have developed a combretastatin-A-4-phosphate (CA4P) resistant variant of SW1222 human colorectal carcinoma cells to examine the relative importance of vascular versus tumor cell targeting in the ultimate treatment response. SW1222Res cells were generated through exposure of wild-type cells (SW1222WT) to increasing CA4P concentrations *in vitro*. Increased resistance was confirmed through analyses of cell viability, apoptosis and multidrug-resistance (MDR) protein expression. *In vivo*, comparative studies examined tumor cell necrosis, apoptosis, vessel morphology and functional vascular end-points following treatment with CA4P (single 100 mg/kg dose). Tumor response to repeated CA4P dosing (50 mg/kg/day, 5 days/week for 2 weeks) was examined through growth measurement, and ultimate tumor cell survival was studied by *ex vivo* clonogenic assay. *In vitro*, SW1222Res cells showed reduced CA4P sensitivity, enhanced MDR protein expression and a reduced apoptotic index. *In vivo*, CA4P induced significantly lower apoptotic cell death in SW1222Res versus SW1222WT tumors indicating maintenance of resistance characteristics. However, CA4P-induced tumor necrosis was equivalent in both lines. Similarly, rapid CA4P-mediated vessel disruption and blood flow shut-down were observed in both lines. Cell surviving fraction was comparable in the two tumor types following single dose CA4P and SW1222Res tumors were at least as sensitive as SW1222WT tumors to repeated dosing. Despite tumor cell resistance to CA4P, SW1222Res response *in vivo* was not impaired, strongly supporting the view that vascular damage dominates the therapeutic response to this agent.

Keywords: combretastatin, vascular targeting, drug resistance, tumor

Vascular disrupting agents (VDAs) are a relatively new group of therapeutic agents designed to target the tumor vasculature, causing vascular collapse, blood flow shut-down and subsequent tumor cell death.¹⁻³ Low molecular weight microtubule depolymerizing agents represent the largest family of this class of agent, the most widely investigated of which is disodium combretastatin A-4 3-O-phosphate (CA4P).⁴ CA4P, currently in Phase II/III clinical trials,^{2,5} is a soluble phosphate pro-drug derivative of the natural parent compound combretastatin-A-4 (CA4) and is distantly related to colchicine.^{6,7} Preclinical studies have shown that CA4P causes a catastrophic disruption of tumor blood flow, which is evident within the first few minutes of drug administration. Extensive hypoxia, secondary to CA4P-induced blood flow reduction, culminates in hemorrhagic tumor cell necrosis by 24 hr.^{8,9} CA4P and other VDAs are highly selective for rodent and human tumors where they cause significantly greater vascular damage compared with normal tissues.⁸⁻¹² The mechanisms through which VDAs elicit their anti-tumor activity are conceptually different from those of classic chemotherapeutic agents that directly target the tumor cell component and kill cells by apoptosis or related mechanisms.¹³ Although the precise molecular pathways that drive tumor vascular collapse are not yet fully understood, *in vitro* analyses have shown that VDAs act through binding to tubulin resulting in microtubule depolymerization, triggering morphological changes in endothelial cells that include increased blebbing and contraction, contributing to the disruption of cell-to-cell junctions and increased permeability.¹⁴⁻¹⁷ These endothelial cell responses are rapid and can be extrapolated to at least

partially explain observations *in vivo*: an extensive rapid drop in tumor blood flow and collapse of established tumor vasculature^{4,8,18–20} and an increase in tumor vascular permeability.^{18,21,22}

In addition to their targeted effects on endothelial cells, tubulin binding agents are established anti-cancer therapeutics with direct cytotoxic effects on tumor cells *per se*.²³ *In vitro*, CA4P inhibits tumor cell proliferation and causes mitotic arrest by interfering with mitotic spindles and chromosome attachment.^{24–28} These effects are dependent on both level and duration of drug exposure. Mitotic-arrested cells subsequently undergo mitotic catastrophe and apoptosis through caspase-dependent and -independent mechanisms. *In vivo*, the plasma half-life of the active CA4 is short^{11,29} and it is difficult to predict whether drug exposures are great enough for significant direct cytotoxic effects to occur under these conditions, especially as there may be a degree of drug trapping within tumor tissue, as a consequence of vascular collapse. To maximize efficacy and achieve local tumor control, it is necessary to combine vascular disrupting agents with other therapeutic approaches such as conventional chemotherapy or radiotherapy.² Consequently, it is vital to understand drug effects on both the vascular and tumor cell compartments, to optimize treatment combinations and scheduling. Dong *et al.*³⁰ showed that CA4P resulted in an increase in GRP78, a protein associated with drug resistance. Thus, as has been documented with multiple other therapeutic agents, treatment with CA4P might result in development of multidrug resistance (MDR) through increased expression of efflux pump proteins such as P-glycoprotein (P-gp) and multidrug resistance-associated protein 1 (MRP1) in remaining viable tumor cells. These efflux pumps prevent intracellular drug accumulation and as a consequence could confer resistance to subsequent treatment with secondary drug-based agents.³¹

Here, we have developed a variant of the wild type human colorectal carcinoma SW1222 cell line (SW1222^{WT}) with resistance to CA4P (SW1222^{Res}). Following confirmation of altered expression of MDR efflux pumps and corresponding sensitivity to CA4P *in vitro*, we have carried out a series of comparative studies *in vivo* where we considered both the vascular disrupting and direct anti-tumor effects of CA4P. We hypothesized that if direct cytotoxic effects of CA4P on tumor cells contributed to therapeutic outcome then this would translate as a reduced response in the resistant line. We compared levels of CA4P-induced vascular shut-down and tumor cell necrosis and apoptosis after a single dose of the drug in SW1222^{WT} and SW1222^{Res} xenografts. We also performed growth delay studies to ascertain the relative contribution of vascular *versus* direct cytotoxic activities of CA4P in determining response to therapy.

Material and Methods

Development of the CA4P resistant SW1222 cell line

The human colorectal carcinoma SW1222 cell line, a kind gift from Dr. Barbara Pedley, was selected for this study, as its response to CA4P has been well characterized.^{32,33} Cells were maintained in DMEM supplemented with 10% fetal calf serum. To generate resistance, cells were initially exposed to 5 nM CA4P for 2 weeks; this was then increased in 10 nM increments on a weekly basis to 100 nM. Thereafter, cells were exposed to CA4P at 100 nM increments, until a final concentration of 5 μ M was reached. Cells were maintained in 5 μ M CA4P to preserve resistance for over 3 months before use. When implanted into immunocompromised mice, SW1222 cells

form tumors with a characteristic glandular morphology,³⁴ a characteristic also of the resistant line.

Measurement of *in vitro* cell sensitivity to CA4P

Sensitivity of SW1222^{WT} and SW1222^{Res} cells to CA4P was quantified by studying cell proliferation and viability. SW1222^{WT} or SW1222^{Res} cells were plated in 12-well culture plates (1 x 10⁵ cells per well). CA4P was then added in fresh media 24 hr later. Viable cells were counted using a Vi-Cell Cell Viability Analyser (Beckman-Coulter, UK) at various times after

CA4P. In some experiments specific MRP inhibitor, MK571³⁵ (Calbiochem, Merck Biosciences, UK) was added to the cells together with CA4P.

Western blot analysis

To study expression of MDR proteins, extracts from confluent SW1222^{WT} or SW1222^{Res} cells were prepared in Biosource Cell Extraction Buffer (Invitrogen, Paisley) supplemented with 1 mmol/L phenylmethanesulfonyl fluoride, and CompleteTM protease inhibitor cocktail (Roche Diagnostics, UK). Equal amounts of protein were separated on NuPAGE 7% Tris-acetate gels (Invitrogen), transferred to nitrocellulose membranes and probed with antibodies to MRP1 (1:500 dilution; Enzo Life Sciences UK) or P-gp (1:800 dilution; Sigma, UK). Immunoreactive bands were visualized by ECL (GE Healthcare, UK). To confirm equal loading, blots were reprobed for actin (1:2,000 dilution; Sigma, UK).

Establishment of tumors and CA4P treatment

SW1222^{WT} or SW1222^{Res} cells were injected subcutaneously (5×10^6 cells in 50 μ l serum-free DMEM) into the rear dorsum of 8–12-week-old female SCID mice obtained from an in-house breeding program. For monitoring tumor growth, three orthogonal tumor diameters (d1, d2 and d3) were measured using calipers and tumor volume was calculated using the formula $0.52 \times d1 \times d2 \times d3$. CA4P, kindly provided by Professor Bob Pettit, was dissolved in saline as a 10 mg/ml stock and administered *in vivo* by intra-peritoneal injection at 50 or 100 mg/kg, once mean tumor diameter reached 5–6 mm. Control mice received equal volumes of saline. Tumor-bearing animals were weighed at regular intervals and monitored for evidence of drug-induced toxicity. All animal procedures were carried out in accordance with U.K. Animals (Scientific Procedures) Act 1986 and following local ethical approval.

Assessment of ex vivo tumor cell viability

To examine *ex vivo* tumor cell sensitivity to CA4P, tumors were enzymatically digested (0.05% pronase, 0.04% DNase and 0.025% collagenase) to a single cell suspension, and seeded into culture flasks. Once confluent, cells were subcultured into 12-well plates, and treated with CA4P 24 hr later. Viable cell counts were performed 24–144 hr after the start of CA4P treatment.

Assessment of tumor necrosis and vessel morphology

For assessment of necrosis, tumors were excised 24 hr post-treatment, fixed in formalin and embedded in paraffin. Sections from the centre of each tumor were stained with haematoxylin and eosin (H&E) and necrosis was quantified over the entire tumor section using an ocular Chalkley grid and a 20x objective (mean number of points per tumor: 1,850 \pm 149). Chalkley counts were calculated as the proportion of points on the grid overlying necrotic tissue, measured in adjacent regions of interest over the entire tumor section. Blood vessel endothelial cells were identified in formalin fixed sections by staining with rat anti-mouse CD31 antibody (1:300 dilution; BD Pharmingen) followed by biotinylated anti-rat IgG (1:200 dilution, Vector Laboratories, UK). Signal amplification was achieved using streptavidin-horseradish peroxidase (Vector Laboratories) followed by Biotinyl Tyramide Amplification Reagent (TSATM Biotin System, NEL700, Perkin Elmer) according to the manufacturer's instructions. Immunoreactive cells were visualized with DAB. Stained sections were counterstained with haematoxylin to allow visualization of tissue architecture.

Measurement of tumor cell apoptosis

Apoptotic cell death *in vitro* was measured using an ELISA-based photometric assay kit (Cell Death Detection ELISA^{PLUS}, Roche Diagnostics, UK) as we described previously.³⁶ Briefly, cells seeded in 24-well plates were allowed to adhere overnight and then treated with CA4P for 24 hr. Cytoplasmic fractions were analyzed for nucleosome generation according to the manufacturer's

instructions. An increase in optical density over that of control untreated cells was represented as “fold increase” in released nucleosomes. For assessment of apoptotic cell death *in vivo*, formalin fixed tumor sections were stained using the ApopTag plus peroxidase *in situ* apoptosis detection kit (Millipore, UK) as per the manufacturer’s instructions. This kit follows the same principle as the TUNEL assay, using terminal deoxynucleotidyl transferase enzyme to label DNA fragments in apoptotic cells. Apoptosis was also assessed in tumor sections by immunostaining for active caspase-3, using anti-cleaved caspase-3 (Asp175) antibody (1:2,000 dilution; Cell Signaling, New England Biolabs, UK) as previously described.³⁷ Apoptotic cells were quantified using a 10 x 10 ocular graticule (total area 1 mm²) using a 20x objective in 5 random fields of view, avoiding necrotic regions. Data were expressed as the mean number of apoptotic cells/mm².

Measurement of clonogenic survival

Clonogenic survival assays were performed using established protocols.³⁸ Briefly, excised tumors were enzymatically dissociated (0.05% pronase, 0.04% DNase and 0.025% collagenase) to a single cell suspension. Dilute cell suspensions were plated in triplicate in 100 mm tissue culture plates. Colonies were stained ~21 days later with 0.1% methylene blue and those containing 50 or more cells were counted. The plating efficiency (PE) was calculated as the total number of colonies/number of cells seeded. The surviving fraction (SF) was calculated taking into account the size of the tumor and number of cells extracted according to the following formula: (PE of CA4P treated tumor/the mean PE of all control tumors) (number of cells extracted g⁻¹ of CA4P treated tumor/the mean number of cells extracted g⁻¹ of all control tumors).

Measurement of relative red cell flux

Red blood cell (RBC) flux was monitored using the Oxford Array multiple channel laser Doppler system (Oxford Optronics, Oxford, UK). Mice were anaesthetized using iso-fluorane and kept warm using a thermostatically controlled heating pad in a heated chamber. Three or four microprobes were inserted into each tumor and once readings were stabilized for 20 min CA4P was administered. RBC flux was monitored continuously for 60 min and for at least 5 min following a lethal pentobarbitone injection to obtain measurement of the biological zero RBC flux. Readings were recorded every 10 sec, and 100 sec averages were calculated for each probe. Because of variation in the absolute values of individual probes, data were normalized against the initial pretreatment readings for each probe following subtraction of the biological zero reading.

Analysis of vascular density and vessel perfusion

Vessel perfusion was calculated as the ratio of perfused to total vessel area, as identified by pixels positive for administered lectin and endogenous CD31, respectively. FITC-conjugated lectin (Vector Laboratories) (0.5 mg/ml in saline; 200 II) was injected i.v. 24 hr post-treatment with CA4P and 5 min before sacrifice. Tumors were rapidly excised, frozen in OCT, cryostat-sectioned, and stained by immunofluorescence for endothelial cell marker CD31 using rat anti-mouse CD31 monoclonal antibody (1:500 dilution; BD Pharmingen) as we described previously.³⁹ Images of perfused vessels (lectin) and total vessels (CD31) were acquired using a Leica AF6000 inverted microscope. For each tumor, 10–12 random fields were imaged, using a 20x objective over 2 tumor levels sectioned 200–300 μ m apart. The total area in pixels of lectin and CD31 staining was assessed for each image using in-house developed image-analysis software^{40,41}, which allowed selection of individual thresholds for each fluorescence channel of a representative image from each tumor. The optimal thresholds were then applied to all images acquired for an individual tumor. Perfusion was calculated as the ratio of lectin to CD31 staining 100. Vascular density was calculated as the total area of CD31 staining per tumor area.

Statistical analyses

Experiments with three or more groups were analyzed for statistical significance using the Kruskal-Wallis analysis of variance, and individual comparisons within these groups were carried out using Dunn's test. Experiments with two groups were analyzed for statistical significance using the Mann-Whitney statistical test. In all cases, differences between groups were described as significant if the probability corresponding to the appropriate statistic was <0.05 .

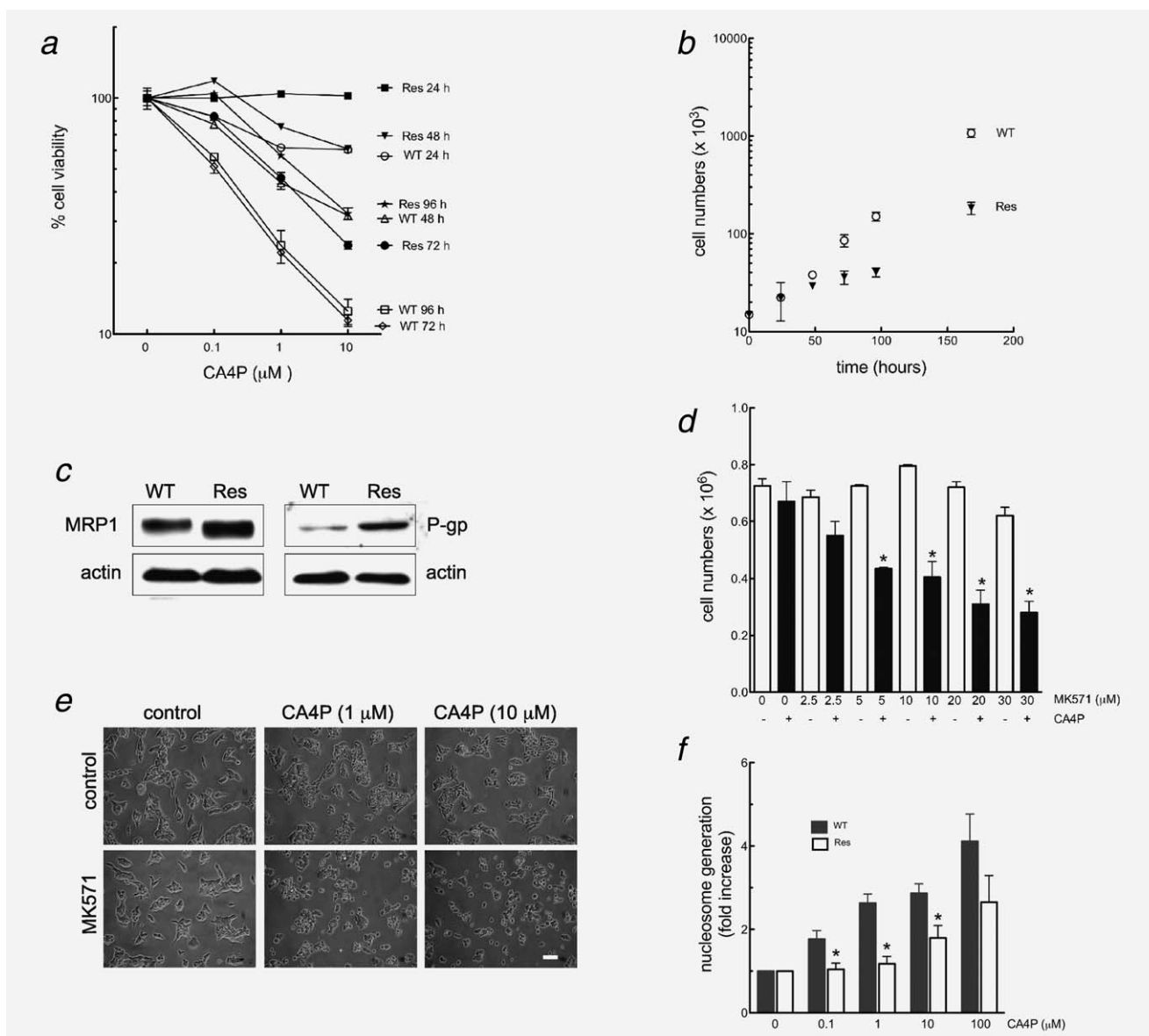


Figure 1. The SW1222^{Res} line demonstrates reduced sensitivity to CA4P *in vitro*. (a) Mean number of viable tumor cells \pm SEM ($n = 3$), normalized against untreated controls, are shown following *in vitro* exposure to CA4P for 24 to 96 hr. (b) Growth curves of SW1222^{WT} and SW1222^{Res} cells *in vitro* ($n = 3$). (c) Representative western blots demonstrating relative expression levels of MRP1 and P-gp normalized to actin. (d) SW1222^{Res} cells were treated with MRP1 inhibitor MK571 6 h before CA4P for 24 hr. Values represent mean number of viable tumor cells \pm SEM ($n = 3$). “*” indicates significance ($p < 0.05$). (e) Representative images of SW1222^{Res} cells, 24 hr after CA4P \pm MK571, demonstrating reversal of resistance. (f) Apoptotic nucleosome degradation 24 hr after CA4P. Values are mean absorbance over untreated controls \pm SEM ($n = 3$). “*” indicates significance ($p < 0.05$).

Results

The SW1222^{Res} line demonstrates reduced sensitivity to CA4P *in vitro*, associated with enhanced expression of MDR proteins. Differences in sensitivity to CA4P between SW1222^{WT} and SW1222^{Res} lines were established through assessment of cell growth and viability following exposure to increasing concentrations of CA4P for 24–72 hr. The SW1222^{Res} line was less sensitive to CA4P relative to the SW1222^{WT} line (Fig. 1a).

Exposure to 1–10 IM CA4P for 24 hr was not cytotoxic to SW1222^{Res} cells, whereas a 72 hr exposure did induce cell death but to a lesser extent than in the SW1222^{WT} line (Fig. 1a). It is of note that, although the SW1222^{Res} line grew successfully *in vitro*, the rate of growth was reduced relative to the SW1222^{WT} variant (Fig. 1b).

Drug resistance is classically achieved through upregulation of MDR proteins, which act to pump cytotoxic agents out of the cell. We examined the expression levels of efflux proteins, MRP1 and P-gp. Both proteins were upregulated in the SW1222^{Res} line relative to the SW1222^{WT} variant (Fig. 1c). To establish whether resistance to CA4P was a consequence of increased efflux pump activity, SW1222^{Res} cells were exposed to the selective MRP1 inhibitor, MK571. MK571 (at doses between 5 and 30 IM) re-established cell sensitivity to CA4P, whereas alone had no effect on basal levels of cell growth and viability (Figs. 1d and 1e). These data suggest that enhanced MRP1 expression contributed significantly to resistance development in the SW1222^{Res} line.

Previous *in vitro* studies have shown CA4P-mediated cytotoxicity to be a result of mitotic arrest and apoptosis.^{26–28} Tumor cell apoptosis was examined in both lines following treatment with CA4P for 24 hr. Consistent with the tumor cell viability data, the SW1222^{WT} tumor line exhibited a dose dependent increase in apoptosis at all CA4P doses tested (0.1–100 IM). In addition, little or no change in basal apoptosis levels was observed in the SW1222^{Res} cells after 0.1 and 1 IM CA4P, whereas the extent of apoptosis induction observed in response to 10 and 100 IM was less than that exhibited by the SW1222^{WT} line (Fig. 1f).

SW1222^{Res} tumors grow successfully *in vivo* and tumor cells maintain reduced sensitivity to CA4P. The SW1222^{Res} line grew successfully *in vivo*; however, time to palpation was notably longer than the WT cells (Fig. 2a), consistent with the reduced proliferation rate of the resistant cells *in vitro*. Once tumors attained a size of 100 mm³, tumor growth was comparable between the two lines, probably reflecting vascularization. During tumor growth *in vivo*, the SW1222^{Res} cells could not be maintained under the selective pressure of CA4P. Therefore, we examined whether tumor cell resistance was maintained *in vivo* by extracting tumor cells from both tumor types and measuring cell viability following exposure *ex vivo* to different doses of CA4P. Analogous to the *in vitro* data described above (see Fig. 1a), cells extracted from SW1222^{Res} tumors maintained their increased resistance to CA4P (Fig. 2b).

SW1222^{Res} tumors demonstrate comparable responses with a single dose of CA4P *in vivo* as SW1222^{WT} tumors

SW1222 is a well-differentiated tumor of glandular morphology (Fig. 3a) with blood vessels surrounding the glands (arrows in Figs. 3a and 3b). The SW1222^{Res} line exhibited a similar glandular morphology *in vivo* with only a few necrotic cells occupying less than 10% of the tumor sections (Fig. 3c). Consistent with the published literature,^{32,33} treatment with a single dose of 100 mg/kg CA4P induced extensive necrosis at 24 hr, identified by H&E staining (Fig. 3a). Necrosis was characterized by large central tumor regions of contiguous cells with pyknotic nuclei that stained homogeneously dark with haematoxylin. Necrotic regions were also

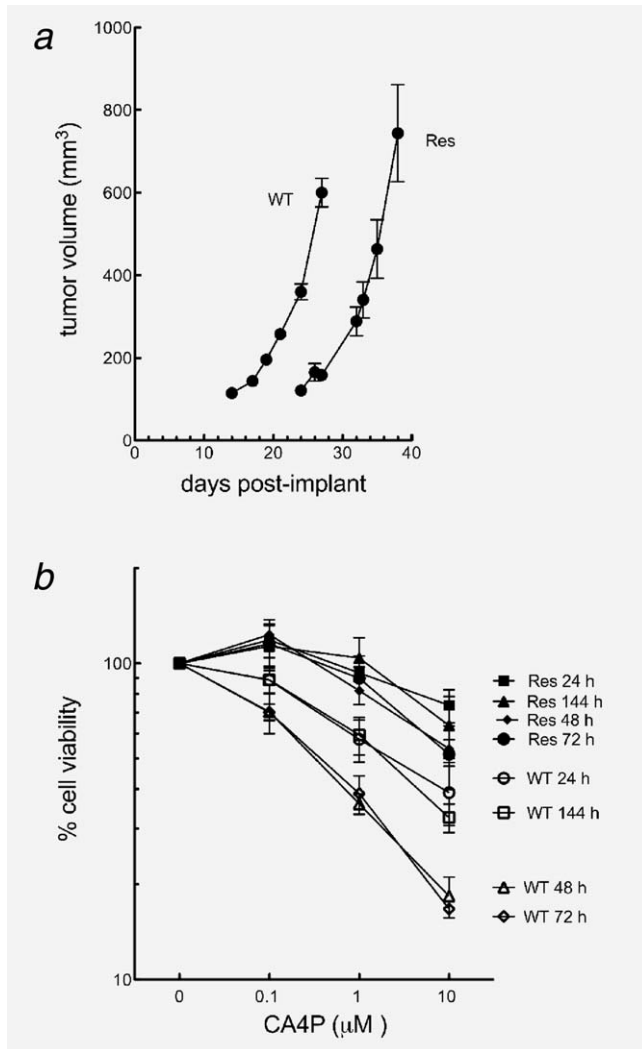


Figure 2. The SW1222^{Res} line demonstrates a slower rate of growth *in vivo*, and maintains reduced sensitivity to CA4P. (a) Tumor growth curves (tumor volume, mm³) are shown for SW1222^{WT} and SW1222^{Res} lines *in vivo* ($n = 6$). (b) Mean numbers of viable cells \pm SEM ($n = 3$) normalized against untreated controls are shown following *in vitro* exposure to CA4P for 24–144 hr of *ex vivo* tumor cells.

characterized by significant thinning of the cell cytoplasm, disruption of tissue architecture and loss of cell-to-cell contact (see inset Fig. 3a). Levels of CA4P-induced necrosis were comparable in the two tumor types (Fig. 3c). Staining of tumor sections for the endothelial marker CD31 revealed severely disrupted, fragmented and collapsed blood vessels within necrotic regions of CA4P-treated tumors (Fig. 3b). Distorted endothelial cells with cytoplasmic protrusions into the lumen were also apparent, even in the non-necrotic regions (Fig. 3b).

Laser Doppler measurement of relative red cell flux was used to assess early CA4P-mediated vascular effects. CA4P treatment significantly reduced relative red cell flux in both lines (Fig. 4a). This was apparent within 10 min of drug administration and continued gradually over the course of a 60 min observation period. There were no significant differences in this early vascular response between the two tumor lines. Functional changes in the vasculature of each tumor type were also assessed at 24 hr after treatment by injecting fluorescent lectin, a marker of perfusion, 5 min before tumors were excised (Fig. 4b). Perfusion, expressed as a ratio of lectin positive pixels over total CD31 positive pixels, was significantly reduced in both tumor lines after CA4P (Fig. 4c) demonstrating that SW1222^{Res} tumors, similar to their wild type counterparts, exhibited classic VDA-mediated vascular functional changes. As for the early vascular effects on red blood cell flux, perfusion changes were also not significantly different between the two tumor lines.

Vascular density, established through measurement of CD31 positive staining in frozen sections, was not significantly different between the two tumor types and remained constant 24 hr after CA4P (Fig. 4d).

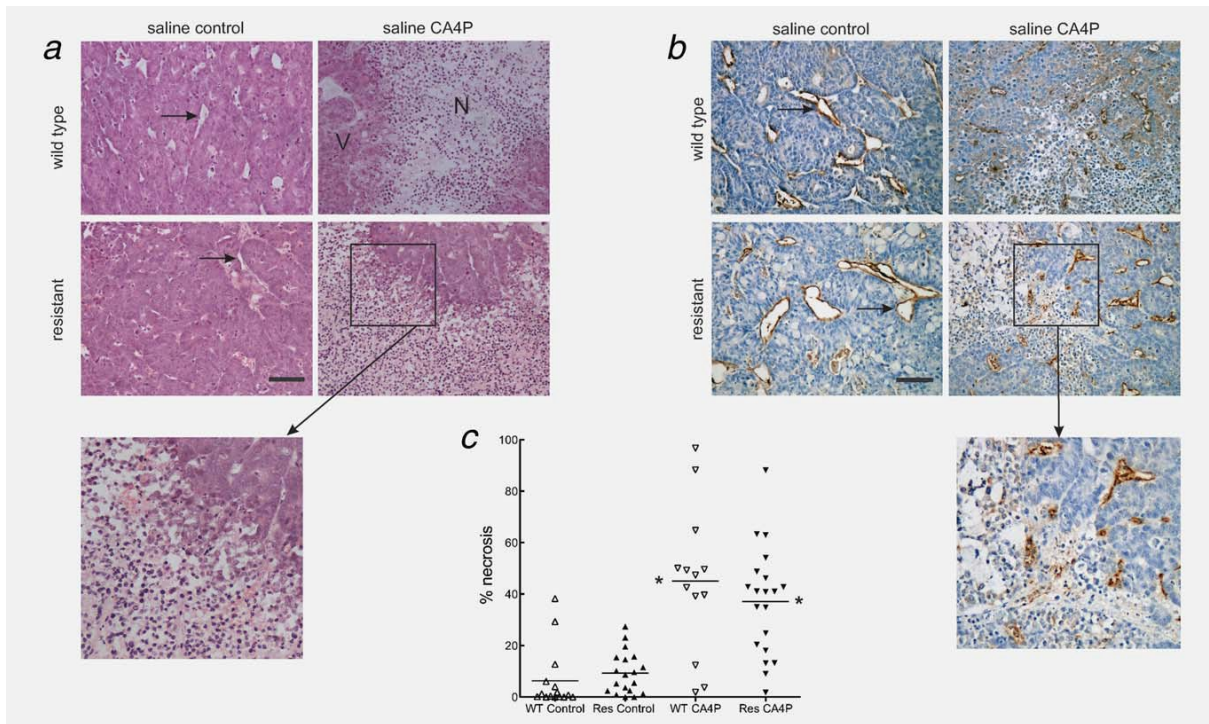


Figure 3. CA4P induced necrosis is comparable between SW1222^{WT} and SW1222^{Res} tumors. (a) Representative H&E staining shows well-differentiated tumors with glandular morphology. Arrows indicate blood vessels surrounding the glands. CA4P (100 mg/kg, 24 hr) caused profound central tumor necrosis. V and N indicate viable and necrotic tissues, respectively. Bar, 100 μ m. (b) Representative CD31 staining shows vessel disruption in necrotic areas. Bar, 200 μ m. (c) Percentage of tumor necrosis is shown for individual tumors. The bar represents the median; “*” indicates significance relative to corresponding control untreated groups ($p < 0.05$).

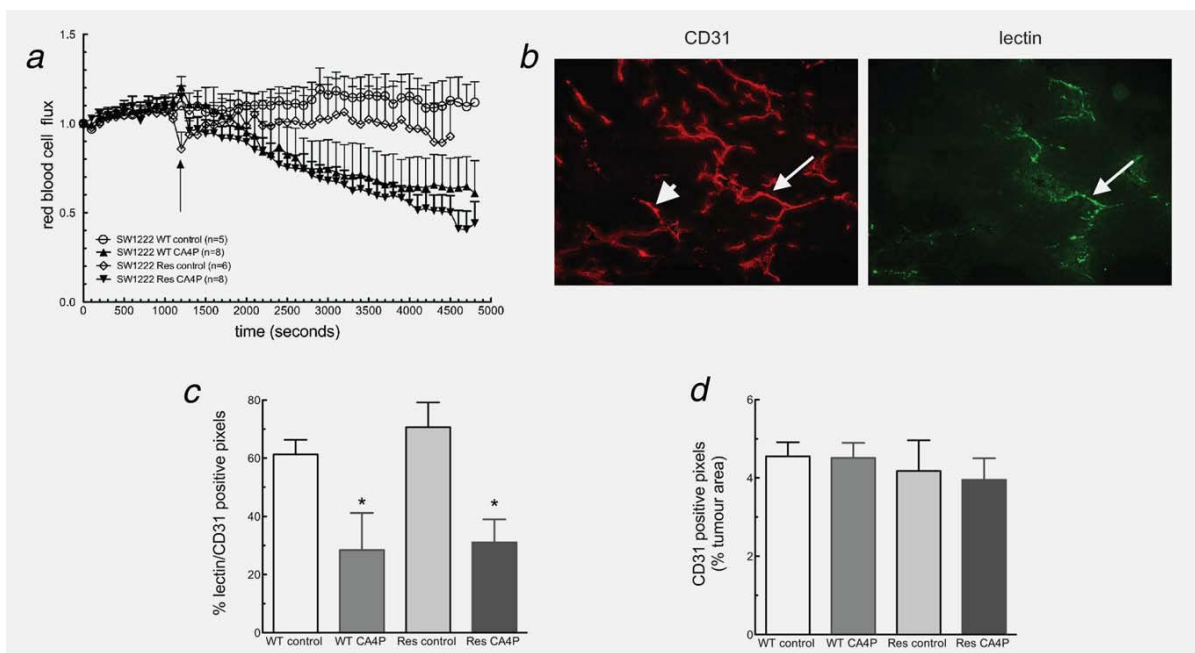


Figure 4. CA4P mediated vascular shut-down is comparable between the SW1222^{WT} and SW1222^{Res} tumors. (a) Mean relative red cell velocity 6 SEM was measured using laser Doppler following treatment with saline control or CA4P. Values were normalized against pretreatment readings for each group. Arrow indicates the start of CA4P (100 mg/kg) or saline administration. (b) Representative immunofluorescence images of CD31 staining (Texas red) and lectin (FITC) demonstrating regions of perfused (arrow) and nonperfused (arrow-head) vessels. (c) Vessel perfusion as the ratio of lectin to CD31 positive pixels in tumors after CA4P (100 mg/kg) or saline control for 24 hr. Values are means 6 SEM. (d) CD31 positive staining, expressed as percentage of total tumor area. In (c) and (d), $n \approx 7$, except for SW1222^{Res} controls where $n \approx 6$. “*” indicates significance relative to control untreated groups ($p < 0.05$).

The surviving tumor cell fraction was examined using a clonogenic survival assay, which accounts for the overall effects of the drug, both vascular and directly cytotoxic. The surviving fraction 24 hr after CA4P did not differ between the two lines (Fig. 5a). Tumor sections were also examined for evidence of apoptotic cell death assessed by staining for DNA fragmentation and for activated caspase-3. In both tumor types, spontaneous levels of apoptosis were comparable (Figs. 5b–5e). Significantly more apoptotic cells were detected in the SW1222^{WT} than the SW1222^{Res} tumors following treatment with CA4P (Figs. 5b–5e). These data confirmed that the SW1222^{Res} cells remained resistant to CA4P when grown as xenografts *in vivo*.

SW1222^{Res} tumors demonstrate comparable response with extended CA4P treatment *in vivo* as SW1222^{WT} tumors

In order to determine whether the reduced apoptotic index observed in the SW1222^{Res} tumors relative to SW1222^{WT} tumors, following single dose CA4P (Fig. 5) translates into a reduced growth response after extended treatment, growth delay was examined in both tumor lines treated with CA4P at 50 mg/kg/day (5 days/week over 2 weeks). CA4P caused a moderate growth delay in both tumor lines, with the SW1222^{Res} tumors displaying at least equivalent sensitivity to their WT counterparts (Fig. 6a). Therefore, the reduced direct cytotoxic action of CA4P against SW1222^{Res} tumors did not translate into an altered tumor growth response, demonstrating that direct cytotoxicity was not the principal mechanism for drug action in a clinically relevant dosing strategy. Interestingly, there was even a tendency for the SW1222^{Res} tumors to grow more slowly in response to CA4P than the SW1222^{WT} tumors, although this did not reach statistical significance with the numbers used (Kruskall-Wallis analysis of variance for tumor volume on day 12). Tumor-bearing animals did not show any evidence of drug-induced toxicity over the course of CA4P treatment (Fig. 6b).

Discussion

This study compared a CA4P resistant tumor line with its wild-type variant to specifically examine the relative importance of the vascular *versus* direct cytotoxic effects of the tubulin binding agent, CA4P.⁴ There is a clear need to distinguish between the overall contribution of these two vital tumor compartments to treatment outcome to maximize the efficacy of combination therapies. In this study we carried out an extensive series of *in vivo* analyses to address this issue. Despite demonstrably significant differences in sensitivity to CA4P *in vitro* and *ex vivo*, tumors propagated *in vivo* from SW1222^{Res} cells were found to behave in a manner comparable to that of SW1222^{WT} tumors, with both variants showing CA4P-induced tumor necrosis, vascular shut-down and similar growth

response. These data demonstrate the dominant role of CA4P mediated vascular effects on therapeutic efficacy.

Tumor cell lines resistant to analogues of CA4 have been developed previously. Nihei *et al.*⁴² found that a colon carcinoma line, resistant to AC-7739 (the active form of AC-7700, now the Sanofi-Aventis compound AVE8062) *in vitro*, was equal to its wild-type counterpart in terms of tumor size after treatment relative to untreated controls, at the time of maximum response. Although this result is consistent with our findings, full growth curves were not shown and no further analyses were performed. Another study used a cervical carcinoma line resistant to CA4 analogue BRP0L075 to examine changes in gene expression related to tumor cell death *in vitro*⁴³ but no *in vivo* investigations were reported.

The SW1222^{Res} line was successfully generated through exposure to increasing concentrations of CA4P, following established procedures.⁴⁴ *In vitro* analyses showed that SW1222^{Res} cells were notably more resistant to CA4P, most likely through elevated expression of MDR proteins, MRP1 and P-gp. Resistance to CA4P was reversed by an inhibitor of MRP1 suggesting that this efflux pump was largely responsible for the developed resistance. The SW1222^{Res} cell line *in vitro* exhibited a clear resistance to CA4P compared with the SW1222^{WT} line at concentrations of 0.1–10 IM for various times. These drug exposures are relevant for *in vivo* studies,

where mouse plasma levels of the active CA4P metabolite CA4 were reported in the region of 0.5–2.8 IM, within

90 min of administering 100 mg/kg CA4P.^{29,45} Our data confirmed several previous studies^{24–28} showing that the mode of direct tumor cell death was anti-proliferative, leading to apoptosis, and that resistance to CA4P was indeed maintained *in vivo*, since markers of apoptosis, namely DNA fragmentation and cleaved caspase-3 expression were significantly greater in SW1222^{WT} compared with SW1222^{Res} tumors following CA4P treatment (see Fig. 5). In addition, *ex vivo* analyses of tumor cell viability demonstrated that SW1222^{Res} tumors maintained their reduced sensitivity to CA4P following growth *in vivo*.

CA4P treatment induced a significant increase in necrosis (40–50% of tumor area) in both SW1222^{WT} and SW1222^{Res} tumors, consistent with its effects in a range of other tumor

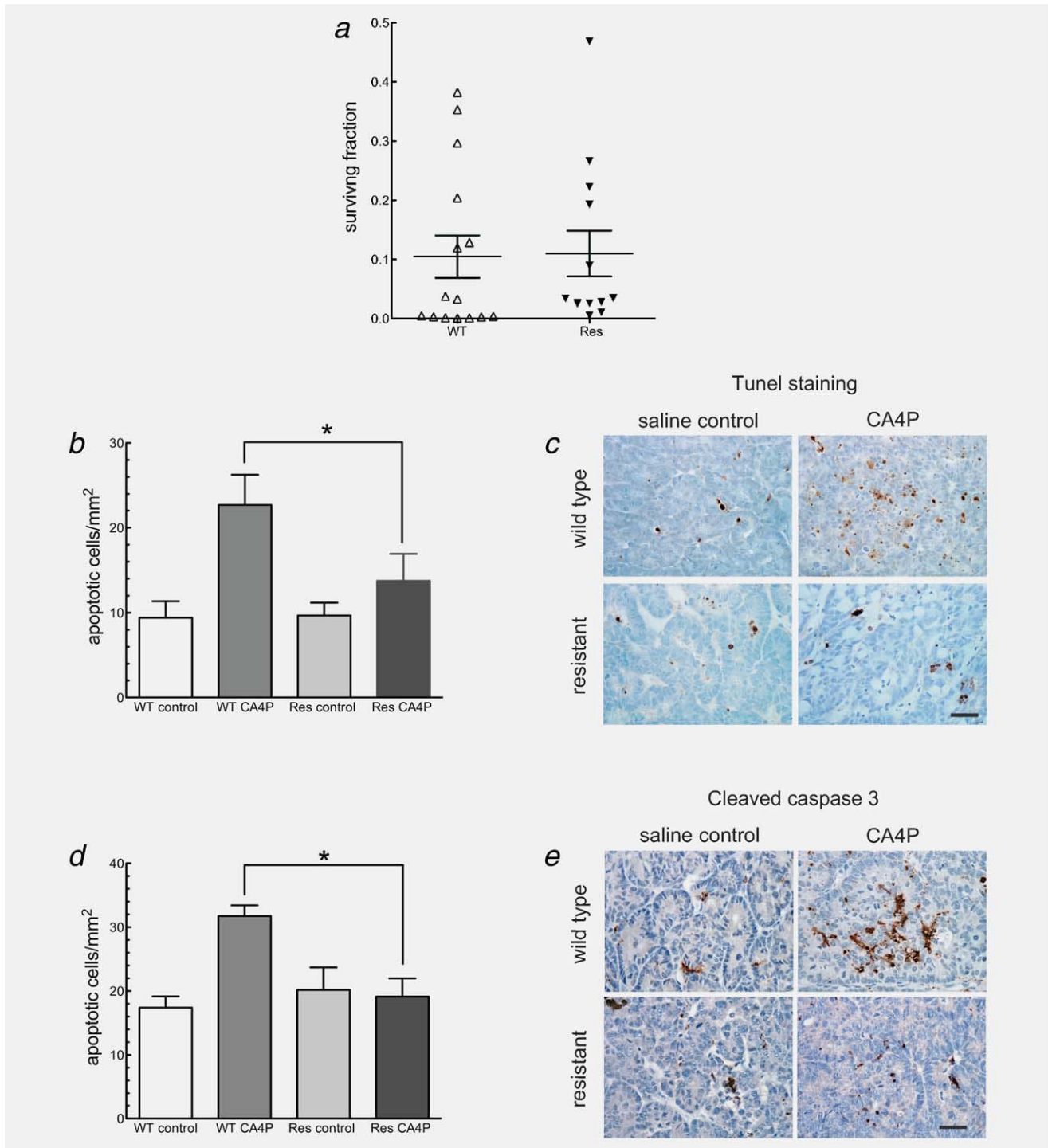


Figure 5. Tumor cell surviving fraction is comparable in both lines following treatment with CA4P, whereas tumor cell apoptosis is reduced in the SW1222^{Res} line. (a) Surviving tumor fraction was measured by clonogenic assay after CA4P (100 mg/kg, 24 hr) or saline control. The bar indicates the median. The mean number of apoptotic cells per mm² were determined by TUNEL assay (b) and cleaved caspase-3 immunostaining (d) in formalin fixed sections. Error bars represent SEM. “*” indicates $p < 0.05$ significance. Representative images of TUNEL staining and cleaved caspase-3 positive cells in SW1222^{WT} and SW1222^{Res} tumors are shown in (c) and (e). Bar, 200 μ m.

model systems.^{8,9,46} Characteristically, VDA-induced necrosis is primarily confined to central tumor regions of contiguous cells, surrounded by a rim of viable tumor cells. This pattern of tumor cell death is distinct from apoptosis and typical of the effects of prolonged vascular

occlusion (ischemia).⁴⁷ Profound CA4P-mediated tumor ischemia has also been shown to be associated with depletion of high energy nucleoside triphosphates,⁴⁸ suggesting that the associated cell death is

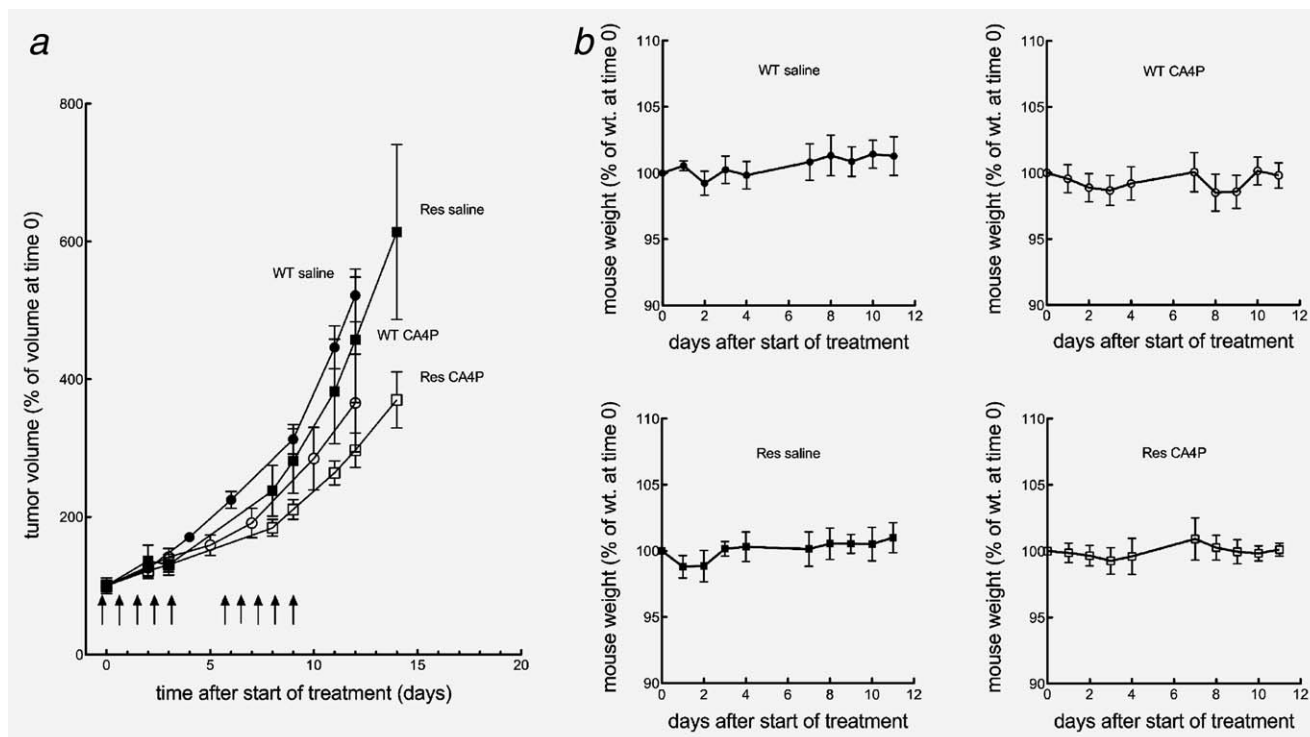


Figure 6. The SW1222^{Res} tumors are as sensitive to continuous CA4P treatment *in vivo* as SW1222^{Res} tumors. (a) Mean tumor growth (relative to tumor volume at treatment start) is shown for SW1222^{WT} and SW1222^{Res} tumors. CA4P was administered at 50 mg/kg/day for 5 days/week over a 3-week period shown by the arrows. Values represent means \pm 6 SEM; $n = 6$ for all groups; (b) Animal weights (relative to weight at start of treatment). Animals implanted with SW1222^{WT} tumors: 22.8 g \pm 60.37 g mean starting weight, 22.8 g \pm 60.31 g mean finishing weight. Animals implanted with SW1222^{Res} tumors: 21.9 g \pm 60.49 g mean starting weight, 21.9 g \pm 60.56 g mean finishing weight.

instigated by a passive process, a feature that distinguishes necrosis from apoptosis. Tumor blood vessel morphology (CD31 staining patterns), blood-flow (laser Doppler flowmetry) and vessel perfusion (lectin binding) were all severely compromised by CA4P treatment to a similar degree in both tumor types, providing compelling evidence for an acute, profound and sustained vascular damage in response to CA4P in both tumor types. The established link between ischemia and necrosis strongly supports the notion that equivalent levels of vascular damage in the SW1222^{WT} and SW1222^{Res} tumors led to the development of equivalent levels of necrosis, *via* ischemia, irrespective of any direct drug-induced cytotoxicity on the tumor cells themselves. It should be noted that endothelial cell death may contribute to the net overall vessel disruption observed in our tumor models^{24,36,49} but is not a prerequisite and cannot explain the early collapse in blood flow that manifests within minutes of drug administration. Therefore, we did not explicitly investigate endothelial cell death either by apoptosis or necrosis in these studies but rather the morphological changes in endothelial cells that potentially compromise blood flow. It should also be noted that there were no intrinsic differences between vascular development in the two lines, which were seen to be equally well vascularized and perfused with similar rates of growth once established.

When we examined overall cell survival of tumor cells following a single 100 mg/kg dose of CA4P to tumour-bearing mice, using a clonogenic assay, we found very similar surviving fractions for the SW1222^{WT} and SW1222^{Res} tumors, despite the reduction in drug-induced apoptosis observed in the SW1222^{Res} tumors. This indicates that the apoptosis levels observed were insufficient to influence overall cell survival and that the necrosis induction was therefore the predominant influence. The constant similarity in response observed *in vivo* between the SW1222^{WT} and SW1222^{Res} tumors strongly supports the concept of a dominant vascular response in mediating treatment outcome *via* necrosis. In reaching this conclusion, we need to consider whether other stromal components could cause significant CA4P-induced tumor cell death. *In vivo* CA4P triggers an influx of immune cells such as neutrophils into the tumor,⁴⁶ which could certainly contribute to tumor cell cytotoxicity. However, these effects are secondary to vascular damage, with immune cells clustering around necrotic tumor regions (our own unpublished data) and so cannot be considered to play an independent role. SW1222^{Res} tumors showed a reduced early growth rate *in vivo* compared with SW1222^{WT} tumors, as shown by the longer time to palpation. Interestingly, a reduced growth rate in drug-resistant tumor lines has been described previously.⁵⁰ This was attributed to elevated caveolin-1 expression in resistant cells,

which has been linked to increased apoptosis.⁵¹ In our study, there was no difference between apoptosis levels in size-matched untreated SW1222^{WT} and SW1222^{Res} tumors, but CA4P more effectively induced apoptosis in SW1222^{WT} compared with SW1222^{Res} cells. Zhao *et al.*⁵² found that over-expression of caveolin-1 blocked TRAIL-induced apoptosis in human hepatocarcinoma cells. Thus, we can speculate that the reduced growth rate of our SW1222^{Res} line and the direct tumor cell response to CA4P is linked to caveolin-1 expression. Further studies would be needed to investigate this hypothesis.

A clear therapeutic concern is that continued exposure to VDAs could induce tumor cell resistance. To address this, we examined tumor growth in response to repeated exposure to CA4P over 2 weeks, where the wild-type tumor cell population might be expected to have a greater impact on the overall response to treatment due to increased drug exposure. However, this was not found to be the case, with the SW1222^{Res} tumors being at least as sensitive as the SW1222^{WT} tumors. Any increase in sensitivity of the SW1222^{Res} tumors compared with the SW1222^{WT} tumors is difficult to interpret, considering that the vascular response after a single dose of CA4P was very similar in the two lines. It is possible that necrotic tissue is cleared more rapidly in the SW1222^{Res} tumors.

Irrespective of the explanation, this result is encouraging, demonstrating that incurred tumor cell resistance to CA4P does not translate to reduced therapeutic efficacy. However, if resistance is acquired through upregulation of MDR proteins, it might impact on response to combined treatment with therapeutic agents that target the tumor cell population directly and this would need further study.

To conclude, we have shown that the SW1222^{Res} tumor line, which was shown to be less sensitive to CA4P with a reduced apoptotic index, responds to CA4P treatment in a manner analogous to that of the SW1222^{WT} tumor line. These data strongly support a dominant role for the vascular targeting effects of CA4P in eliciting an anti-tumor effect, even for repeated dosing strategies. This result is encouraging, suggesting that incurred resistance to CA4P would not impact on its clinical efficacy.

Acknowledgements

We thank Professor Bob Pettit for supplying CA4P and Professor Barbara Pedley for supplying the SW1222^{WT} cell line and protocols for caspase-3 immunostaining. We also thank Mr. Manoj Valluru for help with immunostaining and staff at the Gray Cancer Institute and University of Sheffield for the care of the animals.

We thank Cancer Research UK for the funding

References

1. Chaplin DJ, Horsman MR, Siemann DW. Current development status of small-molecule vascular disrupting agents. *Curr Opin Investig Drugs* 2006;7:522–8.
2. Siemann DW, Chaplin DJ, Walicke PA. A review and update of the current status of the vasculature-disabling agent combretastatin-A4 phosphate (CA4P). *Expert Opin Investig Drugs* 2009;18:189–97.
3. Kanthou C, Tozer GM. Microtubule depolymerizing vascular disrupting agents: novel therapeutic agents for oncology and other pathologies. *Int J Exp Pathol* 2009;90: 284–94.
4. Dark GG, Hill SA, Prise VE, Tozer GM, Pettit GR, Chaplin DJ. Combretastatin A-4, an agent that displays potent and selective toxicity toward tumor vasculature. *Cancer Res* 1997;57:1829–34.
5. Tozer GM, Kanthou C, Lewis G, Prise VE, Vojnovic B, Hill SA. Tumour vascular disrupting agents: combating treatment resistance. *Br J Radiol* 2008;81 (Spec No 1): S12–S20.
6. Pettit GR, Singh SB, Hamel E, Lin CM, Alberts DS, Garcia-Kendall D. Isolation and structure of the strong cell growth and tubulin inhibitor combretastatin A-4. *Experientia* 1989;45:209–11.
7. Pettit GR, Temple C, Jr, Narayanan VL, Varma R, Simpson MJ, Boyd MR, Rener GA, Bansal N. Antineoplastic agents Synthesis of combretastatin A-4 prodrugs. *Anticancer Drug Des* 1995;10: 299–309.
8. Tozer GM, Prise VE, Wilson J, Locke RJ, Vojnovic B, Stratford MR, Dennis MF, Chaplin DJ. Combretastatin A-4 phosphate as a tumor vascular-targeting agent: early effects in tumors and normal tissues. *Cancer Res* 1999;59: 1626–34.
9. Malcontenti-Wilson C, Muralidharan V, Skinner S, Christophi C, Sherris D, O'Brien PE. Combretastatin A4 prodrug study of effect on the growth and the microvasculature of colorectal liver metastases in a murine model. *Clin Cancer Res* 2001;7:1052–60.
10. Hori K, Saito S, Kubota K. A novel combretastatin A-4 derivative, AC7700, strongly stanches tumour blood flow and inhibits growth of tumours developing in various tissues and organs. *Br J Cancer* 2002;86:1604–14.
11. Prise VE, Honess DJ, Stratford MR, Wilson J, Tozer GM. The vascular response of tumor and normal tissues in the rat to the vascular targeting agent, combretastatin A-4-phosphate, at clinically relevant doses. *Int J Oncol* 2002; 21:717–26.
12. Galbraith SM, Maxwell RJ, Lodge MA, Tozer GM, Wilson J, Taylor NJ, Stirling JJ, Sena L, Padhani AR, Rustin GJ. Combretastatin A4 phosphate has tumor antivascular activity in rat and man as demonstrated by dynamic magnetic resonance imaging. *J Clin Oncol* 2003;21: 2831–42.
13. Makin G. Targeting apoptosis in cancer chemotherapy. *Expert Opin Ther Targets* 2002;6:73–84.
14. Galbraith SM, Chaplin DJ, Lee F, Stratford MR, Locke RJ, Vojnovic B, Tozer GM. Effects of combretastatin A4 phosphate on endothelial cell morphology in vitro and relationship to tumour vascular targeting activity in vivo. *Anticancer Res* 2001;21: 93–102.
15. Kanthou C, Tozer GM. The tumor vascular targeting agent combretastatin A-4-phosphate induces reorganization of the actin cytoskeleton and early membrane blebbing in human endothelial cells. *Blood* 2002;99:2060–9.
16. Tozer GM, Kanthou C, Baguley BC. Disrupting tumour blood vessels. *Nat Rev Cancer* 2005;5:423–35.
17. Kanthou C, Tozer GM. Tumour targeting by microtubule-depolymerizing vascular disrupting agents. *Expert Opin Ther Targets* 2007;11:1443–57.
18. Tozer GM, Prise VE, Wilson J, Cemazar M, Shan S, Dewhirst MW, Barber PR, Vojnovic B, Chaplin DJ. Mechanisms associated with tumor vascular shut-down induced by combretastatin A-4 phosphate: intravital microscopy and measurement of vascular permeability. *Cancer Res* 2001;61: 6413–22.
19. Goertz DE, Yu JL, Kerbel RS, Burns PN, Foster FS. High-frequency Doppler ultrasound monitors the effects of antivascular therapy on tumor blood flow. *Cancer Res* 2002;62:6371–5.
20. Horsman MR, Ehrnrooth E, Ladekarl M, Overgaard J. The effect of combretastatin A-4 disodium phosphate in a C3H mouse mammary carcinoma and a variety of murine spontaneous tumors. *Int J Radiat Oncol Biol Phys* 1998;42:895–8.

21. Tozer GM, Ameer-Beg SM, Baker J, Barber PR, Hill SA, Hodgkiss RJ, Locke R, Prise VE, Wilson I, Vojnovic B. Intravital imaging of tumour vascular networks using multi-photon fluorescence microscopy. *Adv Drug Deliv Rev* 2005;57: 135–52.
22. Beauregard DA, Hill SA, Chaplin DJ, Brindle KM. The susceptibility of tumors to the antivascular drug combretastatin A4 phosphate correlates with vascular permeability. *Cancer Res* 2001;61:6811–15.
23. Pasquier E, Kavallaris M. Microtubules: a dynamic target in cancer therapy. *IUBMB Life* 2008;60:165–70.
24. Ahmed B, Van Eijk LI, Bouma-Ter Steege JC, Van Der Schaft DW, Van Esch AM, Joosten-Achjanie SR, Lambin P, Landuyt W, Griffioen AW. Vascular targeting effect of combretastatin A-4 phosphate dominates the inherent angiogenesis inhibitory activity. *Int J Cancer* 2003;105:20–5.
25. Bohle AS, Leuschner I, Kalthoff H, Henne-Bruns D. Combretastatin A-4 prodrug: a potent inhibitor of malignant hemangioendothelioma cell proliferation. *Int J Cancer* 2000;87:838–43.
26. Nabha SM, Mohammad RM, Dandashi MH, Coupaye-Gerard B, Aboukameel A, Pettit GR, Al-Katib AM. Combretastatin-A4 prodrug induces mitotic catastrophe in chronic lymphocytic leukemia cell line independent of caspase activation and poly(ADP-ribose) polymerase cleavage. *Clin Cancer Res* 2002;8:2735–41.
27. Cenciarelli C, Tanzarella C, Vitale I, Pisano C, Crateri P, Meschini S, Arancia G, Antoccia A. The tubulin-depolymerising agent combretastatin-4 induces ectopic aster assembly and mitotic catastrophe in lung cancer cells H460. *Apoptosis* 2008;13: 659–69.
28. Petit I, Karajannis MA, Vincent L, Young L, Butler J, Hooper AT, Shido K, Steller H, Chaplin DJ, Feldman E, Rafii S. The microtubule-targeting agent CA4P regresses leukemic xenografts by disrupting interaction with vascular cells and mitochondrial-dependent cell death. *Blood* 2008;111:1951–61.
29. Kirwan IG, Loadman PM, Swaine DJ, Anthony DA, Pettit GR, Lippert JW, 3rd, Shnyder SD, Cooper PA, Bibby MC. Comparative preclinical pharmacokinetic and metabolic studies of the combretastatin prodrugs combretastatin A4 phosphate and A1 phosphate. *Clin Cancer Res* 2004;10: 1446–53.
30. Dong D, Ko B, Baumeister P, Swenson S, Costa F, Markland F, Stiles C, Patterson JB, Bates SE, Lee AS. Vascular targeting and antiangiogenesis agents induce drug resistance effector GRP78 within the tumor microenvironment. *Cancer Res* 2005;65: 5785–91.
31. Eckford PD, Sharom FJ. ABC efflux pump-based resistance to chemotherapy drugs. *Chem Rev* 2009;109:2989–3011.
32. Pedley RB, Hill SA, Boxer GM, Flynn AA, Boden R, Watson R, Dearling J, Chaplin DJ, Begent RH. Eradication of colorectal xenografts by combined radioimmunotherapy and combretastatin a-4 3-O-phosphate. *Cancer Res* 2001;61: 4716–22.
33. Lankester KJ, Maxwell RJ, Pedley RB, Dearling JL, Qureshi UA, El-Emir E, Hill SA, Tozer GM. Combretastatin A-4-phosphate effectively increases tumor retention of the therapeutic antibody, 131I-A5B7, even at doses that are sub-optimal for vascular shut-down. *Int J Oncol* 2007;30:453–60.
34. Richman PI, Bodmer WF. Control of differentiation in human colorectal carcinoma cell lines: epithelial-mesenchymal interactions. *J Pathol* 1988; 156:197–211.
35. Gekeler V, Ise W, Sanders KH, Ulrich WR, Beck J. The leukotriene LTD4 receptor antagonist MK571 specifically modulates MRP associated multidrug resistance. *Biochem Biophys Res Commun* 1995;208: 345–52.
36. Kanthou C, Greco O, Stratford A, Cook I, Knight R, Benzakour O, Tozer G. The tubulin-binding agent combretastatin A-4-phosphate arrests endothelial cells in mitosis and induces mitotic cell death. *Am J Pathol* 2004;165:1401–11.
37. Bressenot A, Marchal S, Bezdetsnaya L, Garrier J, Guillemin F, Plenat F. Assessment of apoptosis by immunohistochemistry to active caspase-3, active caspase-7, or cleaved PARP in monolayer cells and spheroid and subcutaneous xenografts of human carcinoma. *J Histochem Cytochem* 2009;57: 289–300.
38. Kavanagh MC, Tsang V, Chow S, Koch C, Hedley D, Minkin S, Hill RP. A comparison in individual murine tumors of techniques for measuring oxygen levels. *Int J Radiat Oncol Biol Phys* 1999;44:1137–46.
39. Tozer GM, Akerman S, Cross NA, Barber PR, Bjorndahl MA, Greco O, Harris S, Hill SA, Honess DJ, Ireson CR, Pettyjohn KL, Prise VE, et al. Blood vessel maturation and response to vascular-disrupting therapy in single vascular endothelial growth factor-A isoform-producing tumors.

Cancer Res 2008;68:2301–11.

40. Reyes-Aldasoro CC, Griffiths MK, Savas D, Tozer GM. CAIMAN: an online algorithm repository for Cancer Image Analysis, *Comp Meth Prog Biomed*; 2011; 103 (2), 97–103
41. Reyes-Aldasoro CC, Williams LJ, Akerman S, Kanthou C, Tozer GM. An automatic algorithm for the segmentation and morphological analysis of microvessels in immunostained histological tumour sections; *J Microsc*; 2011; 242 (3), 262–278
42. Nihei Y, Suga Y, Morinaga Y, Ohishi K, Okano A, Ohsumi K, Hatanaka T, Nakagawa R, Tsuji T, Akiyama Y, Saito S, Hori K, et al. A novel combretastatin A-4 derivative, AC-7700, shows marked antitumor activity against advanced solid tumors and orthotopically transplanted tumors. *Jpn J Cancer Res* 1999;90:1016–25.
43. Cheung CH, Chen HH, Kuo CC, Chang CY, Coumar MS, Hsieh HP, Chang JY. Survivin counteracts the therapeutic effect of microtubule de-stabilizers by stabilizing tubulin polymers. *Mol Cancer* 2009;8:43.
44. Wehbe H, Kearney CM, Pinney KG. Combretastatin A-4 resistance in H460 human lung carcinoma demonstrates distinctive alterations in beta-tubulin isotype expression. *Anticancer Res* 2005;25: 3865–70.
45. Stratford MR, Dennis MF. Determination of combretastatin A-4 and its phosphate ester pro-drug in plasma by high-performance liquid chromatography. *J Chromatogr B Biomed Sci Appl* 1999;721: 77–85.
46. Parkins CS, Holder AL, Hill SA, Chaplin DJ, Tozer GM. Determinants of antivascular action by combretastatin A-4 phosphate: role of nitric oxide. *Br J Cancer* 2000;83:811–16.
47. Denekamp J, Hill SA, Hobson B. Vascular occlusion and tumour cell death. *Eur J Cancer Clin Oncol* 1983;19:271–5.
48. Beauregard DA, Thelwall PE, Chaplin DJ, Hill SA, Adams GE, Brindle KM. Magnetic resonance imaging and spectroscopy of combretastatin A₄ prodrug-induced disruption of tumour perfusion and energetic status. *Br J Cancer* 1998;77: 1761–7.
49. Iyer S, Chaplin D, Rosenthal D, Boulares A, Li L-Y, Smulson M. Induction of apoptosis in proliferating human endothelial cells by the tumor-specific antiangiogenesis agent combretastatin A-4. *Cancer Res* 1998;58:4510–14.
50. Lavie Y, Fiucci G, Liscovitch M. Up-regulation of caveolae and caveolar constituents in multidrug-resistant cancer cells. *J Biol Chem* 1998; 273:32380–3.
51. Lavie Y, Liscovitch M. Changes in lipid and protein constituents of rafts and caveolae in multidrug resistant cancer cells and their functional consequences. *Glycoconj J* 2000;17:253–9.
52. Zhao X, Liu Y, Ma Q, Wang X, Jin H, Mehrpour M, Cheng Q. Caveolin-1 negatively regulates TRAIL-induced apoptosis in human hepatocarcinoma cells. *Biochem Biophys Res Commun* 2009; 378:21–6.